Resilient Structures and Sustainable Construction
Edited by Pellicer, E., Adam, J. M., Yepes, V., Singh, A., and Yazdani, S.

ISBN: 978-0-9960437-4-8

NUMERICAL PARAMETRIC STUDIES FOR THERMOGRAPHIC INSPECTION IN CONCRETE

RILYA RUMBAYAN[1] and GLENN WASHER[2]

[1]*Dept of Civil Engineering, Manado State Polytechnic, Manado, Indonesia*
[2]*Dept of Civil and Environmental Engineering, University of Missouri, Columbia, USA*

Thermographic imaging technique provides a practical tool for the detection of subsurface delaminations in concrete from a distance without direct access to the surface. In the previous study, a numerical model to predict the thermal contrasts resulting from subsurface voids (i.e., delaminations) in concrete under a given set of environmental conditions was developed using the finite element method. The model was verified using the experimental test data, and the results indicated that the model could be an effective tool to support the thermography inspection of the concrete. In this present study, the use of the verified model to evaluate the effects of other key parameters expected to influence the detectability of the subsurface voids, such as the depth and thickness of a subsurface delamination. The effect of these parameters on the thermal contrast developed on the surface above a subsurface delamination was assessed under a specific set of environmental conditions. The results shown that the maximum thermal contrast decreased exponential by a constant multiple of 0.98 as the void depth increased and the maximum thermal contrast increased nonlinearly with increasing thickness of the void.

Keywords: Delaminations, Subsurface voids, Thermal contrast, Void depth, Void thickness, Thermography.

1 INTRODUCTION

The previous study by the authors was proposed an analytical model of environmental effects on thermal detection of subsurface damage in concrete (Rumbayan and Washer 2014). A 3D, nonlinear, numerical model of transient heat transfer was developed using finite element analysis to examine the environmental effects on thermal response of simulated subsurface voids in a large concrete block. The effects solar radiation, ambient temperature variation, and wind speed on the thermal images of a concrete block model with subsurface voids were presented. The model performance was evaluated by comparing the thermal contrast of the model results with those reported from a previous experiment study (Washer *et al*. 2009). It was found that the model developed was sufficiently accurate to provide a useful tool for predicting the thermal contrasts in response to subsurface in the concrete, and provide a tool to support practical thermographic inspection, for the purpose of improving condition assessments of the existing concrete bridges.

The goal of this study was to evaluate the effects of different key parameters expected to influence the detectability of the subsurface voids in concrete. The objective was to examine the effect of varying void depths and void thicknesses on thermal contrast, to develop a simplified estimation of void depth from the measured thermal contrast.

2 BASIC PRINCIPLES OF THERMOGRAPHY INSPECTION IN CONCRETE

Thermography employs infrared sensors to detect thermal radiation emitted from objects and creates an image of surface temperatures based on the emitted radiation. The energy of emitted radiation is described by the Stefan Boltzmann Law, which stated that the power radiated by a body is directly proportional to the fourth power of its absolute temperature as Eq. (1),

$$q_{rad} = \varepsilon \sigma T^4 \tag{1}$$

in which ε is infrared emissivity of the object, σ is Stefan Boltzmann constant (5.67 x 10^{-8} W m^{-2} K^{-4}), and T is the surface temperature of the object.

In concrete, as shown in Figure 1A, subsurface voids such as delaminations interrupt heat flow producing localized differences in the surface temperature (Maser and Roddis 1990). These localized variations in surface temperature effect the total infrared radiation emitted from the surface. For example, as concrete warms in daytime, the surface temperature of a delamination is higher than the temperature of the sound concrete. The location of subsurface voids can be identified by analyzing the surface temperature variations (Clemena and McKeel Jr 1978, Manning and Holt 1980, Maser and Roddis 1990). These surface temperature variations were examined in terms of thermal contrast, as shown in Figure 1B, to perform quantitative analysis of data in the study. Thermal contrast, ΔT, was defined as Eq. (2),

$$\Delta T = T_{void} - T_{sound\ concrete} \tag{2}$$

where T_{void} is the surface temperature above a void area and $T_{sound\ concrete}$ is the surface temperature in the intact area of the concrete (Washer *et al*. 2009). It can be seen that the thermal contrast curve has a maximum thermal contrast (ΔT_{max}) at a distinct time (t_{max}).

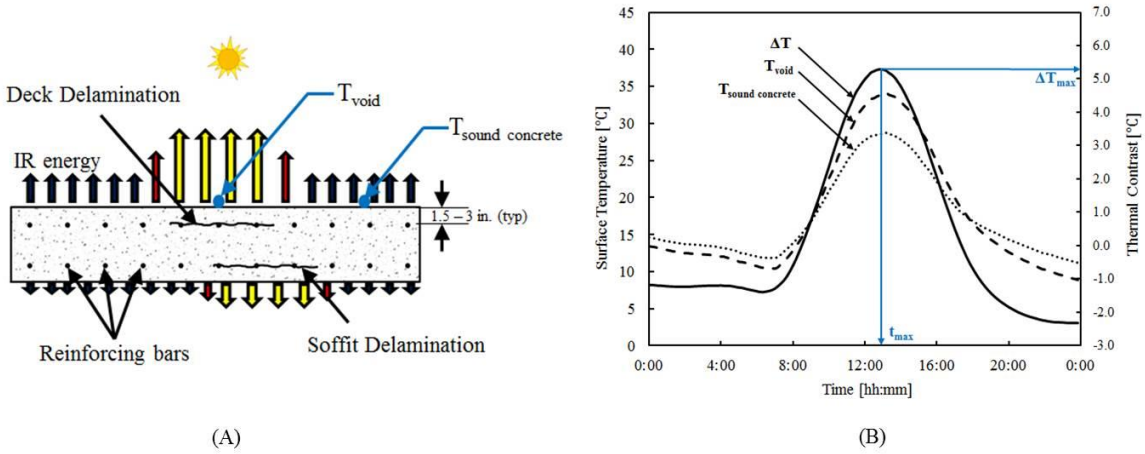

Figure 1. (A) Schematic of the thermography technique to detect a void based on surface temperature differences (i.e., thermal contrast), and (B) Surface temperature and thermal contrast as a function of time (Rumbayan and Washer 2014).

The effective use of quantitative infrared (IR) thermography for subsurface void detection in concrete requires the study of the transient heat transfer phenomenon. Theoretically, this phenomenon could be solved using direct computation of the theory of diffusion or using numerical analysis.

The theory of diffusion in isotropic homogeneous material is governed by the Fourier equation (Lienhard V and Lienhard IV 2011) as Eq. (3),

$$\frac{\partial T}{\partial t} = \alpha \cdot \nabla^2_{x,y,z} T \tag{3}$$

in which $\alpha = k/\rho C_p$ is the thermal diffusivity which indicates how fast a material changes temperature, k is the thermal conductivity, ρ is the density, C_p is the specific heat, T is the temperature, t is time, and ∇^2 is the Laplacian operator. This equation shows that the temperature at any point in the material changes with time during transient heat flow.

3 NUMERICAL PARAMETRIC STUDIES

The parametric studies were conducted using the Finite Element Method (FEM) to evaluate the effect of key parameters expected to influence the detectability of the subsurface voids, for the purpose of providing an analytical tool to study potential testing procedures of thermography in the field. The FEM was used to perform 3D transient heat transfer analysis of a concrete block with a subsurface void under the actual weather conditions. All analyses were simulated using COMSOL-Multiphysics.

The basic geometry for the case which consists of a concrete block 2.4 m wide by 2.4 m tall and 0.9 m deep with a square void inserted. The void was to simulate a delamination. The thermal properties of air were used to describe the voided area. The depth of the void was 25, 51, 76, and 127 mm from the front surface of the block, the lateral size of the void was taken as 305 mm square and the void thickness was ranging from 0.5 mm to 15 mm.

Three consecutive days of weather data (i.e., solar radiation, ambient temperature, wind speed), that were obtained from the previous experimental study, were simulated as boundary conditions. Solar radiation was simulated only at the front surface of the concrete block. Convective cooling was simulated at the front surface and the bottom surface of the concrete. The four other surfaces were treated as adiabatic.

All simulations were run using a ten minute time step over a period of three consecutive days. The purpose was to allow the concrete block reaching its thermal inertia for transient heat flow. In the further analysis, data results of the final 24 hours in the last day were only used. The initial temperature of the concrete block was taken as same as the initial surface temperature obtained from thermocouple measurement in the experimental test. The model was meshed using tetrahedral meshing feature from the COMSOL. The "extra fine" element size was selected as a balance between computational economy and accuracy in the solution (Rumbayan and Washer 2014).

The result of the simulation gave the transient thermal images for the concrete surface. These thermal images gave data of the surface temperature in response to the weather conditions for different depths of void and different thickness of void. For quantitative analysis, surface temperatures as a function of time from a point above the void (T_{void}) and a reference point where there is no void ($T_{sound\ concrete}$) were compared and these surface temperature differences (i.e., thermal contrast) were calculated using Eq. (2).

Figure 2A illustrates an example of the effect of varying void depths on the thermal contrast produced by an air-filled void (for 13 mm void thickness). The results indicated that increasing depth of void reduced the thermal contrast. The void located near the surface concrete result in maximum thermal contrast and short time for maximum thermal contrast, while deep void result in low maximum thermal contrast and long time for maximum thermal contrast. The thickness of the air-filled void was also found to affect the thermal contrast as shown in Figure 2B (for 51 mm

deep void). It should be noted that these results were appropriate for the simulations under a particular weather condition.

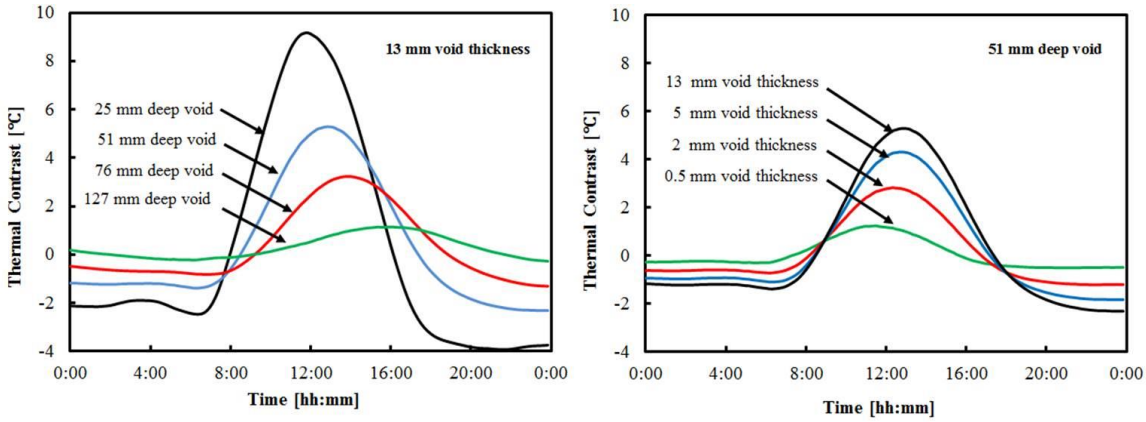

(A) (B)

Figure 2. The time varying thermal contrast: (A) as a function of void depth, and (B) as a function of void thickness.

Figure 3A and Figure 3B present some results of the maximum thermal contrast from voids at various depths and thicknesses, respectively. The results show some interesting details regarding the effect of void depth and void thickness on the thermal contrast. The maximum thermal contrast decreased nonlinearly for increasing void depths (Figure 3A), such as for a void thickness of two mm, the maximum thermal contrast for 25 mm, 51 mm, 76 mm, 127 mm deep void was 4.86°C, 2.82°C, 1.69°C, and 0.69°C, respectively. In addition, Fig. 3B shows that the bigger the void thickness, the better was the thermal contrast. For example, in case of 51 mm deep void, the maximum thermal contrast increased from 1.24°C to 5.29°C with increasing thickness from 0.5 mm to 15 mm.

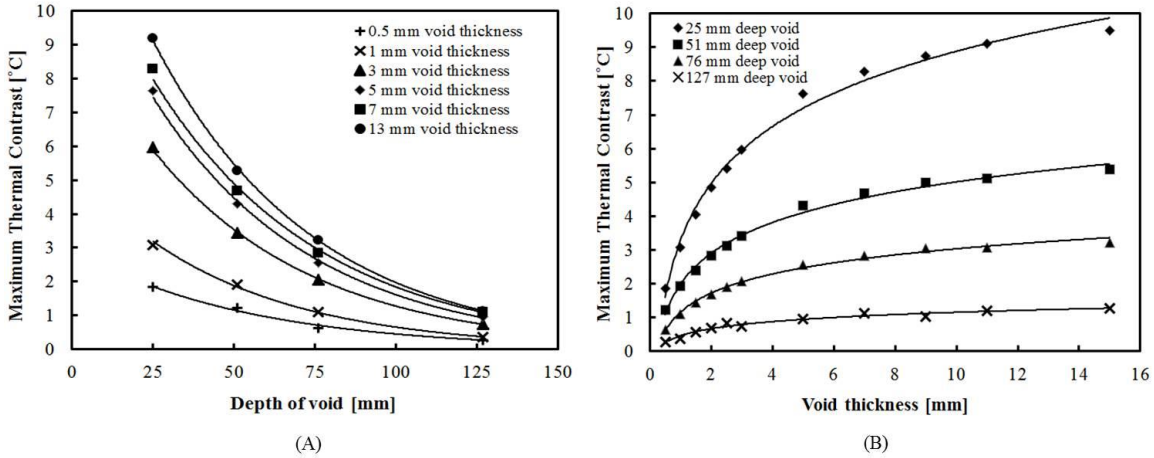

(A) (B)

Figure 3. (A) Effect of void depth on the maximum thermal contrast and (B) Effect of void thickness on the maximum thermal contrast.

The variation of the maximum thermal contrast with void depths could be fitted by the exponential function and the variation of the maximum thermal contrast with void thickness could be fitted by the logarithm functions.

Examining the coefficient of determination (R^2) results for all simulations, the values of R^2 were varied from 0.989 to 0.999. Those values indicate the maximum thermal contrast strongly dependent on void depth that followed the trends of exponential functions as Eq. (4),

$$\Delta T_{max} = A\mathrm{e}^{\mathrm{K}\cdot\mathrm{d}} \tag{4}$$

where ΔT_{max} is the maximum thermal contrast in ℃, d is the depth of void in mm, e is the natural exponential base (e ~2.71828), A and K are constants. Eq. (4) was fitted to the maximum thermal contrast-void depth data in variation of void thickness (z) from 0.5 mm to 13 mm. The best-fit exponential function was obtained by an iterative least-square method.

In this method, the constant, A, determines the maximum thermal contrast when the depth of void was zero for each void thickness. The results of A, as shown in Figure 4A, indicate that A varies due to changes in the void thickness. In general, the values of A increased with increasing void thickness and their relationship could be expressed by the natural logarithm (ln) of z as Eq. (5).

$$A = 3.852\ln(z) + 5.294 \tag{5}$$

The strong dependence between A and the void thickness was indicated by the coefficient of determination of 0.982.

The constant K reflects the rate at which the maximum thermal contrast-void depth curve changes slope and indicates the shape of the curve. Larger values of K lead to faster rates of growth, and vice versa. The results of K, as shown in Figure 4B, indicate that K did not change significantly with increasing void thickness. The average value of K was -0.020 for the void thickness in this study.

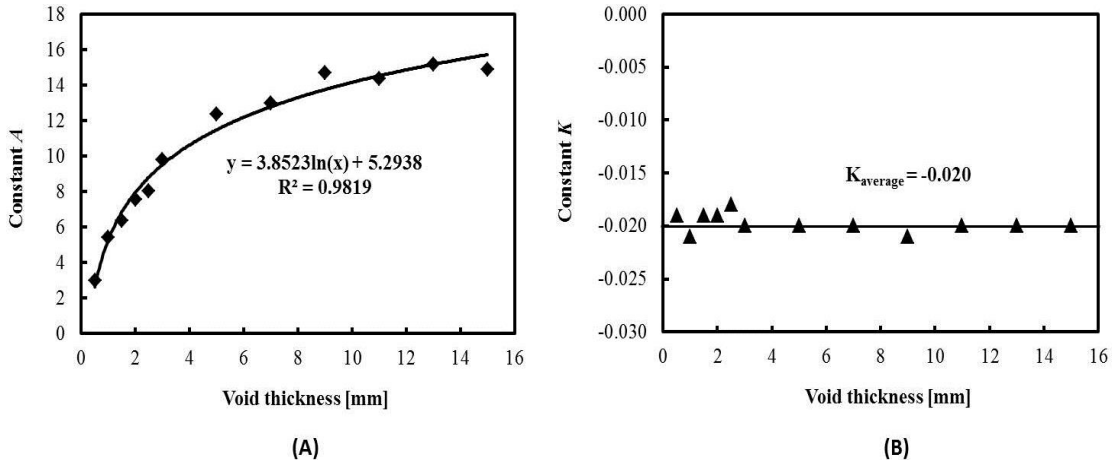

Figure 4. Values obtained for constant A and constant K for exponential expressions fitted to the maximum thermal contrast-void depth data in variation of void thickness.

When the term of e^K in Eq. (4) was replaced by a constant B, as the base of the exponential equation, the value of B could be obtained as 0.980 ($B = e^K = 2.71878^{-0.02} = 0.980$). This means

that the maximum thermal contrast decreased by a constant multiple of 0.980 as the void depth increased over the depth of void range used in the model (25 mm to 127 mm).

Based on the exponential expressions obtained in this case, the relationship between the maximum thermal contrast (ΔT_{max}), void depth (d) and void thickness (z) could be expressed by substituting the value of A in Eq. (5) and the value of B into Eq.(4), therefore

$$\Delta T_{max} = (3.852 \cdot \ln(z) + 5.294) \cdot 0.98^{d} \quad (6)$$

where ΔT_{max} in ℃ and both of d and z in mm.

4 CONCLUSION

This paper focused on the evaluation of the effect of key parameters expected to influence the detectability of the subsurface voids, such as void depth and void thickness. The findings from the study of the effect of varying void depths and void thicknesses demonstrated that the maximum thermal contrasts were a function of both the depth of the void and the thickness of the void. The maximum thermal contrast decreased exponential by a constant multiple of 0.98 as the void depth increased. The maximum thermal contrast increased nonlinearly (as a logarithm function) with increasing thickness of the void. The results also showed that changes in maximum thermal contrast were more pronounced for voids located closer to the surface.

In the future studies, the model proposed will be used to develop a multiple linear regression equation to establish a functional relationship between the thermal contrast at various depths of void and daily environmental parameters. Such the equation could be used to asses if a particular day's weather would produce the thermal contrast required to be imaged using a common thermal camera given the anticipated depth of a delamination and predicted weather conditions.

References

Clemena, G. G. and McKeel Jr, W. T., *Detection of Delamination in Bridge Deck with Infrared Thermography*, Transportation Research Record, 664, 180-182, 1978.

Lienhard V, J. H. and Lienhard IV, J. H., *A Heat Transfer Textbook*, Dover Publications, Mineola, N.Y., 2011.

Manning, D. G. and Holt, F. B., Detecting Delaminations in Concrete Bridge Decks, *Concrete International*, 2(11), 34-41, 1980.

Maser, K. R. and Roddis, W. M. K., Principles of Thermography and Radar for Bridge Deck Assessment, *Journal of Transportation Engineering*, 116(5), 583-601, 1990.

Rumbayan, R. and Washer, G. A., Modeling of Environmental Effects on Thermal Detection of Subsurface Damage in Concrete, *Research in Nondestructive Evaluation*, 25, 235-252, 2014.

Washer, G., Fenwich, R., Bolleni, N., and Harper, J., Effects of Environmental Variables on Infrared Imaging of Subsurface Features of Concrete Bridges, *Transportation Research Record: Journal of the Transportation Research Board*, 2108, 107-114, 2009.